Proc. Natl. Acad. Sci. USA
Vol. 82, pp. 5550–5554, August 1985
Microbiology

Mass distribution of a probable tail-length-determining protein in bacteriophage T4

(virus structure/size regulation/scanning transmission electron microscope/unstained freeze-dried specimens/radial density distribution)

ROBERT L. DUDA*, JOSEPH S. WALL†, JAMES F. HAINFELD†, ROBERT M. SWEET†, AND FREDERICK A. EISERLING*‡§

*Microbiology Department, University of California, Los Angeles, CA 90024; †Biology Department, Brookhaven National Laboratory, Upton, NY 11973; and ‡Molecular Biology Institute, University of California, Los Angeles, CA 90024

Communicated by William B. Wood, April 19, 1985

ABSTRACT **Analysis of dark-field scanning transmission electron micrographs of unstained freeze-dried specimens established that the interior of the intact bacteriophage T4 tail tube contains extra density that is missing in tubes artificially emptied by treatment with 3 M guanidine hydrochloride. The mass of the tail tube is 3.1 × 10^6 daltons, and the central channel is 3.2 nm in diameter. Quantitative analysis of the density data is consistent with the presence of up to six strands of a protein molecule in the central channel that could serve as the template or ruler structure that determines the length of the bacteriophage tail and that could be injected into the cell with the phage DNA.**

A sensitive method using scanning transmission electron microscopy (STEM) combined with digital image processing to generate radial density distributions of macromolecules has been developed recently (1). In this paper, we report the application of this technique to the bacteriophage T4 tail tube, with the goal of learning more about DNA injection and tail length determination.

It is widely accepted that T4 DNA is ejected from the head into the host cell through a central channel in the tail tube (2), yet the evidence is indirect. Disrupted phage particles seen by negative staining in the transmission electron microscope show stain penetration through the tail tube (2), suggesting that it is hollow; phage particles adsorbed to bacteria viewed by both thin sectioning and negative staining show empty heads, contracted tails, and tail tubes still in contact with the cell membrane (3, 4), suggesting that the DNA entered the cell through the tail tube. Studies by low-angle x-ray diffraction of T2 tail tubes reassembled from subunits confirmed the existence of a 3.2- to 3.8-nm diameter central channel (5). Purified tube-baseplates from mutants defective in head and tail sheath production (6) appear "full," in the sense that images of negative-contrast specimens have no stain penetration. In fact, there is no direct evidence that such tubes are filled, since material at the ends could block stain penetration. However, tubes separated from baseplates by guanidine hydrochloride (Gdn·HCl) treatment show partial stain penetration (7), suggesting that a central component is partially removed.

The well-defined length of the T4 tail tube poses another question: how is the length of a stack of identical protein subunits determined? The answer for tobacco mosaic virus (TMV), where the problem was first clearly stated by Caspar (8), and for filamentous DNA bacteriophages (9) is that the length of the structure is determined by a nucleic acid "template" or "ruler" molecule with a fixed genome length. This concept was extended to phage T4 by King (6) to include the possibility that one of the baseplate proteins might instead serve as a ruler for tail tube length. There is another difference between the nucleic acid template models for TMV and filamentous phages and the proposed T4 protein ruler: removal of the nucleic acid requires disassembly of the structure, whereas the T4 protein ruler could, in principle, be ejected with the DNA. An alternative hypothesis, developed by Kellenberger (10) and by Caspar (11) and extended by Wagenknecht and Bloomfield (12) is that length is limited during assembly by a progressively larger deformation of the assembling structure so that, after a certain number of subunits have been added, elongation stops.

Katsura and Hendrix (13) have shown recently that the length of the bacteriophage λ tail is controlled by the length of a minor tail protein, gpH. Viable mutants of λ with in-frame deletions in gene *H* produce phage with proportionally smaller gene *H* proteins and proportionally shorter tails. These findings argue strongly that a protein ruler specifies λ tail length and justify the search for similar template proteins in other systems. The location of gpH in λ tails is not known, but size, stochiometry, and geometric and functional constraints have led Katsura and Hendrix (13) to propose that gpH is inside the tail tube in a six-stranded coiled-coil of mostly α-helical protein.

In the experiments described here, we sought to answer three questions: Is there material inside T4 tube-baseplates? Do the tubes that appear empty by negative staining lack this postulated material? Is such material localized in a particular part of the tube-baseplate? The approach we used was direct mass determination by using STEM.

The STEM produces an image of a specimen by scanning it in a television-type raster with a beam of electrons focused to dimensions as small as 0.25 nm. The electrons scattered into angles representing spacings of 0.015–0.075 nm are collected for each sampling point. Their number, normalized to the total electron beam flux, is an accurate measure of the mass of material in the beam at that point. The two-dimensional array of numerical mass values represents a two-dimensional dark-field image of the specimen. The major sources of random error are the counting statistics of the scattered electrons and nonuniformities in the carbon film used to support the specimen. Systematic errors may arise from artefacts such as impurities in the specimen, residues of nonvolatile salts, or specimen denaturation or proteolysis. Another major source of systematic error is damage to the specimen caused by exposure to the electron beam. Nevertheless, the sensitivity of the method permits accurate measurements even with electron beam doses low enough to prevent significant specimen damage (100–1000 electrons/nm^2). The statistical precision of the integrated mass for an

The publication costs of this article were defrayed in part by page charge payment. This article must therefore be hereby marked "*advertisement*" in accordance with 18 U.S.C. §1734 solely to indicate this fact.

Abbreviations: STEM, scanning transmission electron microscope; Gdn·HCl, guanidine hydrochloride; TMV, tobacco mosaic virus.

§To whom reprint requests should be addressed.

individual molecule of 500,000 daltons is 2% (14). The averaging of measurements made on many molecules will produce values of higher statistical precision.

METHODS

Specimens. Phage growth and sample preparation for purified tube-baseplates and tubes were as described (7), with the difference that the structures were further purified by an additional step using diethylaminoethyl-cellulose ion-exchange chromatography. The STEM studies were carried out at the Brookhaven National Laboratory Biotechnology Resource (15). Procedures for preparation of specimens, especially freeze-drying of unstained specimens at constant pressure and treatment of data for STEM analysis, are described in detail in ref. 16. TMV was added to each sample as an internal mass standard.

Electron Microscopy. The 40-keV electron probe was focused to an effective diameter of 0.25 nm, and images of 512 × 512 picture elements were recorded digitally on magnetic tape using the signal from a large-angle detector (40- to 200-mrad half-angle). Raster sampling time was 8 sec. The magnifications employed produced image fields that covered 0.512 μm on a side. Electron doses were $\approx$300 electrons/nm^2. The liquid nitrogen cold stage maintained a specimen temperature of −150°C in these experiments.

Image Processing. Mass measurements were performed from the digitally recorded data by means of the BNL system of computer programs (17). The techniques for background measurement and mass calibration described in ref. 16 were also employed. Whenever possible, replicate measurements from several areas of a single specimen and from separate specimens were combined not only to improve statistical significance but also to assess the effects of systematic error. STEM images of cylindrical objects such as these tail tubes are projections onto a plane of the density in the cylindrical object. However, one can analyze these images to determine the distribution of density as a function of radial distance from the center of the cylinder. We analyzed several particles from the preparation of tube-baseplates and from the preparation of empty tubes by using procedures developed by Steven and co-workers (1). Individual particles were chosen by visual inspection of the STEM image and the angle of the particle axis was measured very carefully. Density measurements within the cylindrical particle were projected along this axis. The densities were "binned" at intervals that were one-third of the raster sampling of the image, a procedure that partially preserves the 0.25-nm resolution of the electron beam, in spite of the 1-nm sampling. The projected density of each particle was inspected and only symmetric profiles with sharp edges and smooth background were accepted for further processing. A collection of profiles was superimposed by Fourier autocorrelation and averaged by a summing of Fourier coefficients. The summed transforms were smoothed by application of a filter in Fourier space that left coefficients with spatial frequencies of <1.5 nm^{-1} unchanged but decreased smoothly from there to a value of zero at 1.2 nm^{-1}. The profiles were also symmetrized about a central axis and background was subtracted.

Calculation of the radial density distribution depends upon the notion that the particle can be treated as a series of concentric cylindrical shells and that projected density at the periphery of the particle represents only the outer radial shell. Therefore, the density of the projection through the next shell inside the periphery can be "corrected" for the contribution of the outer shell and the density of this next shell can be calculated (1). Thus, in a progressive process one can determine the density of each shell. A consequence of the method is that the density at the innermost radius may be poorly determined. The principal reason for this is that all measurement errors accumulate in the densities calculated for the center. Another is that a tiny fraction of the total mass of the particles is actually near the center; therefore, it is sparsely sampled by the STEM measurement.

RESULTS

Purified tube-baseplates can be partially degraded by treatment with Gdn·HCl to produce tail tubes with the baseplate removed (7). A characteristic of the tube-baseplate is that the tubular region normally appears filled with stain-excluding material. However, in the Gdn·HCl-treated structures, material that filled the tube seems to be absent because electron micrographs show that negative stain can now penetrate at least partly into the region (7). A third type of particle, which appears after several weeks of storage of preparations of the Gdn·HCl-treated tube-baseplates, is a tube with no stain-excluding material left inside. Images were obtained from preparations of all three of these particle types (images of the first two are shown in Fig. 1).

For each particle measured, a zone 28 nm wide was integrated along lengths ranging from 30 to 50 nm (corresponding to 30–50% of the tube length), the length being chosen to include only a segment of the particle that seemed to be uniform in density. For the preparation of the tubes that were freshly treated with Gdn·HCl, a photograph of each image was inspected to choose the particles that seemed to be truly partly filled—that is, those that had one end empty with the other showing material fastened to it with some of this material protruding. The mass per length of each end of these particles was then calculated, with measurements from the two ends being treated separately. The result of these measurements is displayed in Fig. 2 and Table 1.

One can see that the empty end of the Gdn·HCl-treated tubes not only is lower in mass density than either the filled end or the shaft of the tube-baseplates but also is virtually identical to that of the tubes that were seen to be completely empty. Also, the shaft of the tube-baseplates has the highest mass density of any of the particles. Therefore, the material that is present in the tube-baseplates but absent in the empty

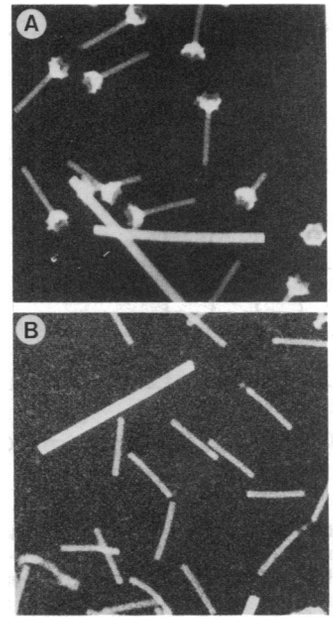

FIG. 1. STEM images of bacteriophage T4 tube-baseplates (*A*) and Gdn·HCl-treated tail tubes (*B*), showing on some particles in *B* the fibrous structure partially released from tail tubes. The tail tubes are $\approx$100 nm long.

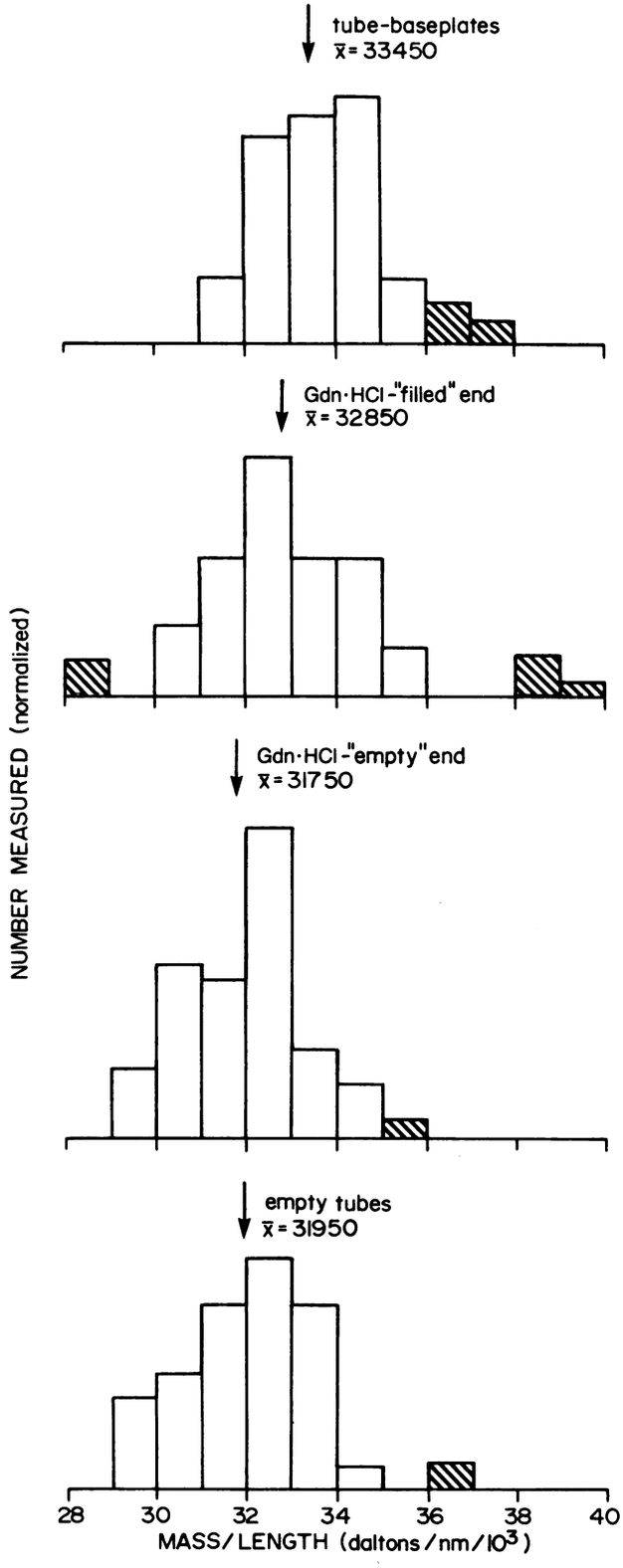

FIG. 2. Frequency of occurrence of mass per unit length values from tube portions of STEM micrographs of T4 tube-baseplates, the filled end of Gdn·HCl-treated tube-baseplates, the empty end of these particles, and empty tail tubes. The numbers of samples in the histograms are 50, 50, 37, and 42, respectively; each is normalized to give the same area under the histogram. Hatched data lay >2 standard deviations from the mean of the rest of the data and were rejected before calculation of the mean values shown in Table 1 and indicated by the arrows.

Table 1. Mean mass per length density values for several particle types after rejection of outliers shown hatched in Fig. 2

Particle type	Mass per length, daltons/nm	Standard deviation		Number of data
		Sample	Mean	
Tube-baseplate	33,450	1050	170	39
Gdn·HCl-treated				
Filled end	32,850	1400	210	45
Empty end	31,750	1300	190	49
Empty tube	31,950	1300	220	36

tubes could have a mass/length ratio as great as 1700 daltons/nm.

Notice that the measured density of the filled end of the Gdn·HCl-treated tubes is intermediate between that of the empty end of this particle and the tube-baseplate shaft. This may be partly because some of the regions included for integration were incompletely filled or partly because this filled end represents a poorly defined intermediate stage in dissociation of the particle.

The mass of unfilled tubes (Table 1) is 3.2×10^4 daltons/nm; using a tube length of 98 nm (18), the estimated mass for the entire tail tube from electron microscopy is 3.1×10^6 daltons. Based on the 6-fold symmetry of the tube (5) and assuming 24 rows of subunits (18), there are 144 subunits per tube. The molecular mass of the tube subunit, gp19, is estimated at 21,000 daltons (19); thus, the predicted tube mass is 3.0×10^6 daltons, in good agreement with the value determined by microscopy.

The STEM measurements can be used to determine the radial position of the material that fills the tail tubes and that is absent from those treated with Gdn·HCl. These calculations were performed as described above. The densities for the untreated tail tubes with baseplates attached and of the (well-aged) empty tubes were projected along the particle axis. The two density profiles are shown in Fig. 3, the higher of the two being from the untreated tubes. Six measurements of filled tubes of total length 267 nm were averaged together, as were 12 measurements of empty tubes with total length of 373 nm. The two curves were scaled together, not to make their outer regions superimpose, but so that their integrals had the values shown in Table 1. The fact that they superimpose so precisely is an indication of the self-consistency of the data and of the fact that the only difference between the

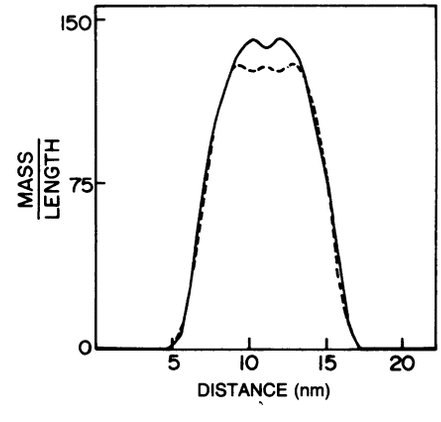

FIG. 3. Mass density profiles summed along the length of tail-tube particles. The upper (solid line) curve is from untreated tail tubes integrated along a length of 267 nm. The lower (dashed line) curve is from aged and apparently empty Gdn·HCl-treated tail tubes integrated along a length of 373 nm. The two curves were scaled for display so that their integrals are in the ratio 33,450:31,950 (see Table 1).

two tube types is in the center. This latter fact is better displayed in the radial density distribution and difference curves shown in Fig. 4. Here the two particles have very similar features at the periphery, including the two maxima at 2.6 and 3.8 nm. Toward lower radius values, however, there is a clear maximum in the difference curve, representing the material removed by Gdn·HCl treatment. Fig. 4 also suggests that the innermost density of empty tubes is greater than full tubes, an apparently spurious result that arises from accumulated errors and limited sampling at the center. The radial density profiles in Fig. 4 can be used to estimate the dimensions of freeze-dried tail tubes. Use of the midpoint between the maximal and minimal density values gives values of 3.2 nm for the central hole diameter and 9.8 nm for the diameter of the tube.

DISCUSSION

Mass determination using STEM methods and radial density distribution analysis was shown recently to be sensitive enough to detect the RNA chain in TMV by comparing TMV with polymers of TMV protein, about a 5% mass difference (1). The dimensions of T-even phage tail tubes have been determined previously by means of x-ray fiber diffraction analysis of partially oriented, hydrated polytubes (5). The diameter of freeze-dried tail tubes found here (9.8 nm) agrees reasonably well with these x-ray results (8.4–9.0 nm) as does the value for the central hole in the tube (3.2 nm vs. 3.4–3.8 nm). Negative-stain measurements using conventional electron microscopy give values of about 9.0–9.5 nm for the diameter and 3.0–3.5 nm for the central hole (5). Given the substantially different methods of specimen preparation and analysis, these results are in good agreement. The STEM also provides an excellent way to determine the molecular weight of the tail tube: using a length of 98 nm, the particle weight of 3.1×10^6 daltons is in excellent agreement with that predicted from other biochemical methods.

One can evaluate the packing of the central tube protein by calculating the dimensions of a single cylinder, and also for six single cylinders, arranged around a central cavity, that could account for its mass. The result (assuming a protein density of 1.35 g/cm^3) is that a single cylinder of protein 1.6 nm in diameter would account for 1700 daltons/nm. Alternatively, six cylinders 0.66 nm in diameter, with a total fiber diameter of 2.0 nm, would also account for this mass. Either of these fibers would clearly fit within the measured internal diameter of the tube.

Previous results (7) showed that Gdn·HCl-treated tubes contain six copies of gp48 (based on dye binding, gel electrophoresis, and baseplate symmetry), suggesting that it might occupy the central channel. Thus, another way to understand the arrangement of protein chains within the tail tube is to estimate the mean number of residues in gp48 (we assume from gel electrophoresis data that the molecular mass of gp48 is about 40,000; using a molecular mass of 110 per residue gives 364 residues). From this we can calculate that for the 364 residues to span the 98-nm tube length, each residue in each chain must extend ≈0.27 nm along the tube, approaching an extended chain or β-type structure. Table 2 shows comparative data for several protein structures.

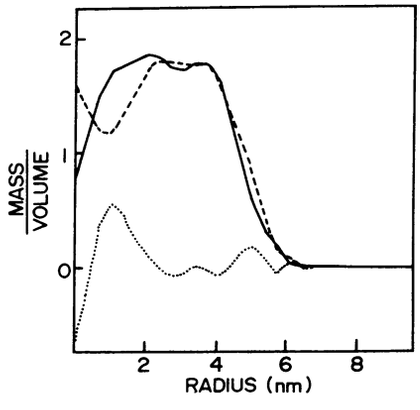

FIG. 4. Profiles of the radial distribution of density in untreated tail tubes (solid line) and Gdn·HCl-treated tubes (dashed line). The difference between these two curves is shown as a dotted line. The difference reaches a maximal value near the center of the tube.

Table 2. Predicted densities for several protein conformations

Structure*	Pitch, nm*	Rise per residue, nm*	Mass per unit length, daltons/nm: One strand	Mass per unit length, daltons/nm: Six strands
α Helix	0.54	0.15	733	4398
3_{10} Helix	0.60	0.20	550	3300
2_7 Ribbon	0.56	0.28	393	2358
β Structures	0.695	0.32–0.34	316	1896

*Data from ref. 19.

The added mass inside the intact tail tubes probably results from several copies of a protein designed to limit the length of the tube during its assembly. gp48 is the next to last protein to be added to the baseplate prior to polymerization of the tube protein gp19 (20) and is a good candidate for the length-determining protein (20). It must, however, be added to baseplates in a globular or compact form during baseplate assembly, since the sedimentation value of the baseplate remains nearly the same after binding gp48 (6, 20) and electron microscopy shows no fiber projecting from baseplates that lack the gp19 tube. Thus, the protein that fills the interior of the tail tube must undergo a major rearrangement and elongation during assembly of the tube protein. Similarly, hydrodynamic properties of the λ tail initiator (outlined in ref. 13) suggest it is a compact structure with a form of gpH that must extend during tail polymerization. Any protein that fills the inside of the tail tube must exit prior to DNA ejection, and this protein might also transmit a signal to the DNA in the head to begin this event (21). It is likely that the length of most phage tails will be found to be determined by a protein template. The length determiner of bacteriophage λ is sufficiently large to span the 150-nm tail length of phage λ in the form of six α helices. The extended-chain conformation described above, approaching that of a β-pleated sheet, is clearly different and possibly reflects an alternate solution to the design problem of a similar biological structure.

We thank Dr. Alasdair C. Steven for help with analysis of the radial density distribution data using his programs at the National Institutes of Health, National Institute of Allergy and Infectious Diseases Laboratory of Physical Biology, Dr. Benes L. Trus, Computer Systems Laboratory, Division of Computer Research Technology, National Institutes of Health, for help with systems and programs, Kristen Chung for STEM sample preparation, and Frank Kito and Mari Gingery for technical assistance. Research support for the T4 work at University of California, Los Angeles, was provided by U.S. Public Health Service Grant AI14092 (to F.A.E.). The STEM facility at Brookhaven is supported by U.S. Public Health Service Grant RR 01777.

1. Steven, A. C., Hainfeld, J. F., Trus, B. L., Steinert, P. M. & Wall, J. S. (1984) *Proc. Natl. Acad. Sci. USA* **81,** 6363–6367.
2. Brenner, S., Streisinger, G., Horne, R. W., Champe, S., Barnett, L., Benzer, S. & Rees, M. W. (1959) *J. Mol. Biol.* **1,** 281–292.
3. Simon, L. & Anderson, T. F. (1967) *Virology* **32,** 279–297.
4. Simon, L. & Anderson, T. F. (1967) *Virology* **32,** 298–305.
5. Moody, M. F. & Makowski, L. (1981) *J. Mol. Biol.* **150,** 217–244.

6. King, J. (1968) *J. Mol. Biol.* **32,** 231–262.
7. Duda, R. & Eiserling, F. A. (1982) *J. Virol.* **43,** 714–720.
8. Caspar, D. L. D. (1960) *Trans. N.Y. Acad. Sci.* **22,** 519–521.
9. Griffith, J. & Kornberg, A. (1974) *Virology* **59,** 139–152.
10. Kellenberger, E. (1972) *Ciba Found. Symp.* **7,** 189–206; 295–299.
11. Caspar, D. L. D. (1980) *Biophys. J.* **32,** 103–135.
12. Wagenknecht, T. & Bloomfield, V. A. (1975) *Biopolymers* **14,** 2297–2309.
13. Katsura, I. & Hendrix, R. (1984) *Cell* **39,** 691–698.
14. Wall, J. S. & Hainfeld, J. F. (1984) in *Forty-Second Annual Proceedings of the Electron Microscopy Society of America*, ed. Bailey, G. W. (San Francisco Press, San Francisco), pp. 154–157.
15. Wall, J. (1979) in *Introduction to Analytical Electron Microscopy*, eds. Hren, J. J., Goldstein, J. I. & Joy, D. C. (Plenum, New York), pp. 333–342.
16. Mosesson, M. W., Hainfeld, J., Wall, J. & Haschemayer, R. H. (1981) *J. Mol. Biol.* **153,** 695–718.
17. Hainfeld, J. F., Wall, J. S. & Desmond, E. J. (1982) *Ultramicroscopy* **8,** 263–270.
18. Eiserling, F. A. (1983) in *Bacteriophage T4*, eds. Mathews, C. K., Kutter, E. M., Mosig, G. & Berget, P. B. (American Society for Microbiology Publications, Washington, DC), pp. 11–24.
19. Dickerson, R. E. & Geis, I. (1969) *The Structure and Action of Proteins* (Harper and Row, New York), p. 32.
20. Berget, P. B. & King, J. (1983) in *Bacteriophage T4*, eds. Mathews, C. K., Kutter, E. M., Mosig, G. & Berget, P. B. (American Society for Microbiology Publications, Washington, DC), pp. 246–258.
21. Goldberg, E. (1983) in *Bacteriophage T4*, eds. Mathews, C. K., Kutter, E. M., Mosig, G. & Berget, P. B. (American Society for Microbiology Publications, Washington, DC), pp. 32–39.